CNWRA *A center of excellence in earth sciences and engineering*

A Division of Southwest Research Institute
6220 Culebra Road • San Antonio, Texas, U.S.A. 78228-5166
(210) 522-5160 • Fax (210) 522-5155

January 13, 2000
Contract No. NRC-02-97-009
Account No. 20-01402-861

U.S. Nuclear Regulatory Commission
ATTN: Mr. Neil M. Coleman
Division of Waste Management
Two White Flint North
Mail Stop 7C 6
Washington, DC 20555

Subject: Transmittal of "Comparison of Numerical and Analytical Models of Unsaturated Flow Around Underground Openings: Considerations for Performance Assessments of Yucca Mountain, Nevada, as a High-Level Nuclear Waste Repository" (IM-01402-861-050)

Dear Mr. Coleman:

This letter transmits Intermediate Milestone 20-01402-861-050 under the title "Comparison of Numerical and Analytical Models of Unsaturated Flow Around Underground Openings, Considerations for Performance Assessments of Yucca Mountain, Nevada, as a High-Level Nuclear Waste Repository." This report provides technical bases for Nuclear Regulatory Commission review of the U.S. Department of Energy (DOE) performance assessments of Yucca Mountain as a potential Geological Repository for nuclear waste.

Water percolating through unsaturated fractured rock and entering waste emplacement drifts is the expected pathway for release of radionuclides to the biosphere. DOE has invested substantial effort attempting to demonstrate the phenomenon of seepage exclusion from underground openings by capillarity. A numerical model of seepage exclusion and flow around drifts provided the basis for the DOE abstraction of seepage into drifts for the Total System Performance Assessment for the Viability Assessment.

While benchmarking the code MULTIFLO Version 1.2 against analytical solutions of seepage exclusion from underground horizontal cylindrical openings, we found substantial error introduced as a result of grid discretization. This problem is caused by sharp saturation and pressure gradients adjacent to the drift wall that require a very finely discretized grid to resolve. An important finding of this work is that these errors tend to be nonconservative. Specifically, the numerical models predicted more seepage exclusion and more capillary diversion than the analytical models. This indicates that DOE numerical models of capillary diversion may be systematically biased towards nonconservative results. The results reported here will directly support revision of the Unsaturated and Saturated Flow under Isothermal Conditions Issue Resolution Status Report.

Washington Office • Twinbrook Metro Plaza #210
12300 Twinbrook Parkway • Rockville, Maryland 20852-1606

If you have any questions regarding this deliverable, please call me at (210) 522-5540 or Dr. Debra Hughson at (210) 522-3805.

Sincerely yours,

English C. Pearcy, Manager
Geohydrology and Geochemistry

cc:
J. Linehan
B. Stiltenpole
B. Meehan
J. Greeves
J. Holonich
W. Reamer
K. Stablein
D. Brooks
B. Leslie
J. Ciocco
D. Esh
R. Codell
W. Patrick
CNWRA Directors
CNWRA Element Managers
T. Nagy (SwRI Contracts)
P. Maldonado

Comparison of Numerical and Analytical Models of Unsaturated Flow Around Underground Openings, Considerations for Performance Assessments of Yucca Mountain, Nevada, as a High-Level Nuclear Waste Repository

Debra L. Hughson
Center for Nuclear Waste Regulatory Analyses
San Antonio, Texas

Richard Codell
U.S. Nuclear Regulatory Commission
Rockville, Maryland

ABSTRACT

While benchmarking the integrated finite-volume code MULTIFLO against the analytical solution of Philip et al. (1989) for cylindrical underground openings, we found numerical simulation of dripping threshold flux consistently higher than the analytical solution for both rectangular and unstructured grids. The magnitude of error is proportional to the alpha parameter characterizing capillarity. This may bias estimates of repository performance towards non-conservatism.

INTRODUCTION

Performance calculations for the proposed repository at Yucca Mountain, Nevada, are sensitive to estimates of water dripping into waste emplacement drifts. In the performance assessment for the Viability Assessment (DOE, 1998), abstraction for seepage flux magnitude and fraction of affected waste packages was based on a 3-D heterogeneous porous continuum representation of flow through the fracture network in Topopah Springs welded tuff. Simulations using the TOUGH code (Birkholzer et al. 1999) showed reasonable agreement with analytical solutions. While testing the integrated finite-volume two-phase water–energy flow and reactive transport code MULTIFLO 1.2β, developed at the Center for Nuclear Waste Regulatory Analyses (Lichtner and Seth, 1998), we benchmarked it against the analytical solution of Philip et al. (1989) for horizontal cylindrical underground openings. This analytical result gives the magnitude of infiltration and deep percolation flux that is the threshold for dripping to occur into the cavity, assuming a homogenous porous medium characterized by an exponential relative permeability model (Gardner, 1958) and steady state flow. The focus of this work is a comparison between the analytical solution and numerical simulations using unstructured and rectangular element grids for varying Gardner α parameter in the relative permeability model. Comparisons were made using a 2-D grid of rectangular elements and an unstructured grid with several refinements of node placement around a circular interior no-flow boundary. Our results indicate that numerical simulations, using both grid types, tend to predict a greater dripping threshold than the analytical solution and that this error increases with increasing α.

MODEL GRIDS

Rectangular Grids

The vertical 2-D grid consisting of 30 elements in the horizontal direction and 40 elements in the vertical direction, with each element a cube 0.5 m on each side, is shown in Figures 1 and 2. A 5 m diameter circular drift, centered between no-flow side boundaries and 7.5 m above the bottom prescribed state boundary, is approximated by using a material property such that capillary pressure $P_c = 0$ for all saturations. For flux to cross the boundary between material properties, the rock

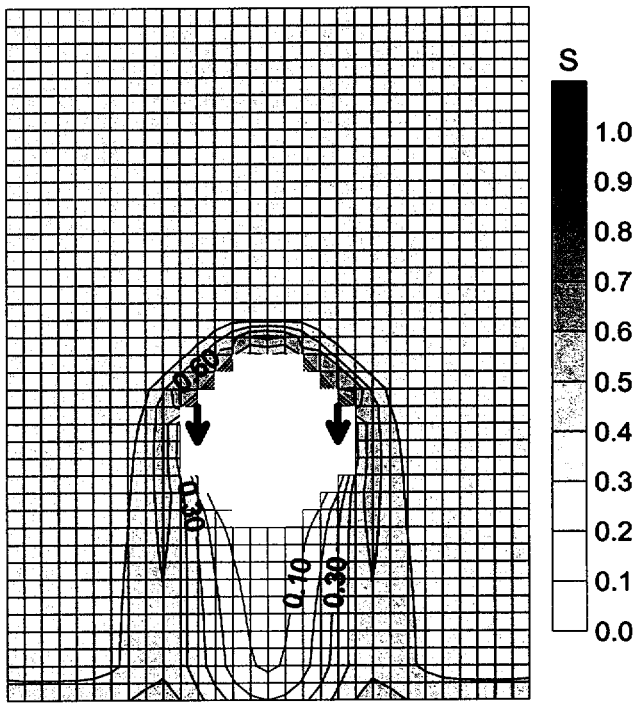

Figure 1. Rectangular element grid 1. Saturation is contoured and arrows denote locations of the first drips.

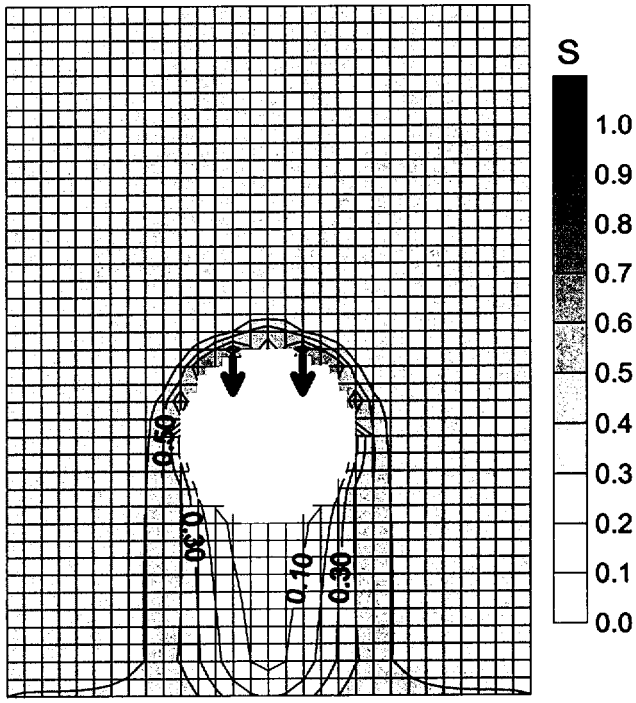

Figure 2. Rectangular element grid 2. Saturation is contoured and arrows denote locations of the first drips.

immediately adjacent to the drift wall must be saturated with a capillary pressure of zero. Gravity then causes flow to cross the boundary and enter the opening. However, since the rock and drift are represented by elements of finite volume, there is a gravitational component of head difference equal to the vertical distance between the nodes of these elements. This causes flux in the discretized domain to cross the material property boundary when capillary pressures in the rock are negative. We examined two different strategies for minimizing the gravitational component of head difference between nodes above and below the drift wall due to element size. The first, used with grid 1 shown in Figure 1, is to assign the connection distance between the boundary and the node above a value of zero and the distance between the boundary and the node below a comparatively small value of 1 mm. Each element of the grid is a cube 0.5 m on a side with a volume of 0.125 m^3, interfacial areas of 0.25 m^2, and distances of 0.25 m from the centered nodes to the interfaces between. Adjustments to node connections made for the second strategy, grid 2, are detailed in Table 1 with reference to Figure 3. For example, the block volume of element number 4 in Figure 3 was reduced to 0.03125 m^3, as indicated by the quarter of element 4 that is shaded. The distances from the node of element 4 to the interface with element 3, and vice versa, were left as 0.25 m but the distance to the interfaces with elements 5 and 7 were set to zero. Likewise the distance from the node of element 5 to the interface with element 4 was left as 0.25 m but the distance from the node of element 7 to the interface with element 4 was set at 0.0001 m. The small connection lengths between nodes result in large conductances between those elements. However, since the drift elements are at residual saturation, "upwinding" results in zero relative permeability while capillary pressures in the rock elements are negative.

Table 1. Nodal connection details for elements defining the drift in grid 2. A and B refer to numbers in Figure 3.

Nodes A–B	A to B (m)	B to A (m)	Area (m^2)	Vol A (m^3)
1–3	0	0.01	0.25	0.125
2–4	0	0.25	0.125	0.125
3–4	0.25	0.25	0.125	0.125
4–5	0	0.25	0.125	0.03125
4–7	0	0.0001	0.125	0.03125
5–8	0	0.01	0.125	0.09375
6–9	0	0.25	0.125	0.125
8–9	0.25	0	0.125	0.125
9–10	0.25	0.25	0.125	0.03125
9–11	0	0.001	0.125	0.03125
11-12	0.25	0.25	0.125	0.125
12–14	0	0.25	0.125	0.09375
13–14	0.25	0	0.125	0.125
14–15	0.25	0.25	0.125	0.03125
14–16	0	0.001	0.125	0.03125

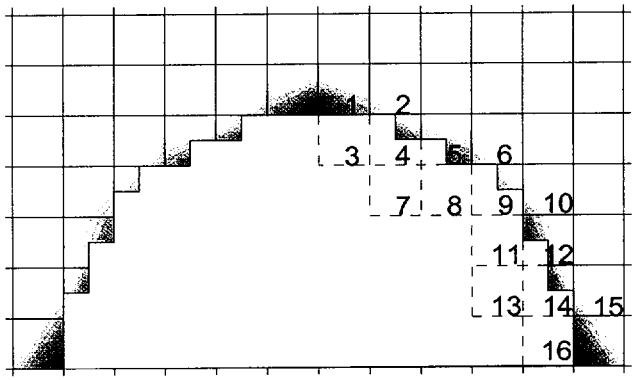

Figure 3. Close up view of the upper portion of the drift in Figure 2. Details of nodal connections for the numbered elements are given in Table 1.

Unstructured Grids

Nodal placements were generated with transcendental functions and further refined by placing rings of nodes slightly larger than the 2.5 m radius interior no-flow boundary. The base-case refinement, grid u0 shown in Figure 4, was to place a ring of nodes at 2.501 m so that the gravitational component of gradient at the drift crown was 1 mm. An additional refinement of 2 rings, one with a radius of 2.55 m and the other 2.6 m, was required to reduce error to a magnitude similar to that of grid 2. The drift in these unstructured grids is represented by a 2.5 m radius circular no-flow boundary made up of 0.01 m segments. Nodal and interfacial dimensions for hexagonal elements were generated using the code AMESH (Haukwa, 1998).

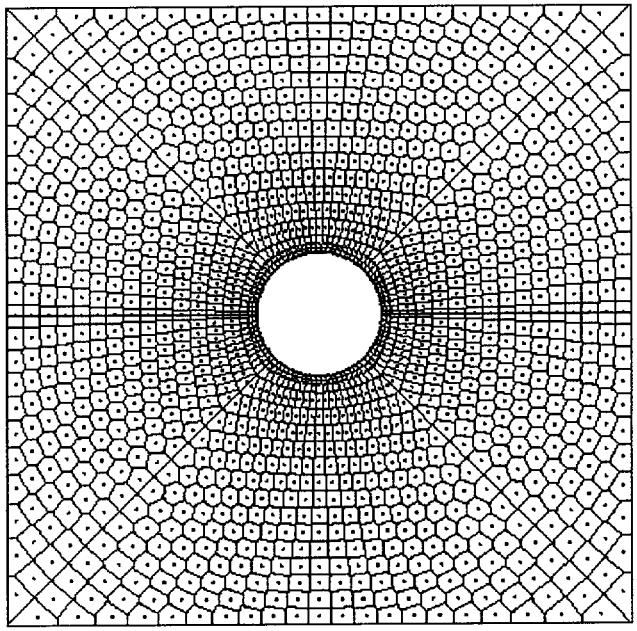

Figure 4. Unstructured grid u0. Side length is 25m. A 5 m diameter internal no-flow boundary represents the drift. Grid u2 has nodes for grid refinement around the drift

RESULTS

Steady state flow was simulated with prescribed flux at the top boundary, prescribed state at the bottom boundary, and no-flow along the sides. Rock permeability was 1.0×10^{-13} m^2 with a porosity of 0.1. Saturation contours at dripping threshold for grids 1 and 2 are shown in Figures 1 and 2 for α = 3.3E-3 Pa^{-1}. Locations in the drift where drips first form are indicated by arrows. Dripping threshold for the rectangular grids 1 and 2 was taken to be the boundary flux that resulted in a non-zero vertical flux vector at the drift wall boundary. For the unstructured grids, dripping threshold was taken to be the boundary flux that resulted in a saturation of 0.9999 for at least one node on the drift wall boundary. With α = 3.3E-3 Pa^{-1} and a drift radius of 2.5m the solution of Philip et al. (1989) for threshold flux is 372.7 mm/yr. Percent error is calculated as

$$Error = \frac{numerical - analytical}{analytical} \times 100$$

Flux into the drift, at the locations indicated by arrows in Figure 1, occurred with a uniform flow condition of 780.3 mm/yr imposed along the top boundary, which is an error of 109%. By adjusting element volumes, interfacial areas, and nodal connections distances, as shown in Table 1, the error was reduced to 49% and drips formed at the locations indicated by arrows in Figure 2 with a flux boundary condition of 556 mm/yr.

For a small pore size distribution parameter of α = 1.0E-5 Pa^{-1}, dripping threshold estimated using the unstructured grid in Figure 4 results in an error of 1.2%. For larger α, however, the error increases substantially reaching 453% for α = 3.3E-3 Pa^{-1}. The inverse of α is approximately equivalent to the height of capillary rise, or the pressure head at which the larger pores de-water. For α=1.0E-5 Pa^{-1}, this is about 10 m and for α = 3.3E-3 Pa^{-1} this is about 0.03 m. Clearly, additional grid refinement is needed to capture the sharp gradient in the 3 cm boundary layer that forms at the drift crown. Adding an extra ring of nodes between the inner ring 1 mm from the inner boundary and the next 0.33 m from the inner boundary decreases error depending on its location. With the extra ring of nodes placed at 0.1 m from the inner boundary, error in simulated dripping threshold was 109%. Further reduction in error, to 49%, was attained by adding yet another ring of nodes at 0.05 m from the inner boundary. Saturation contours at dripping threshold for α = 3.3E-3 Pa^{-1} are shown in Figure 5 for this additional refinement, referred to as grid u2. The arrow in Figure 5 indicates the location where the first drip forms. Dripping threshold flux as a function of α for a horizontal 2.5 m radius cylindrical tunnel in a homogeneous porous medium is shown in Figure 6 compared to the analytical solution. Except for the rectangular element grids 1 and 2 at the small

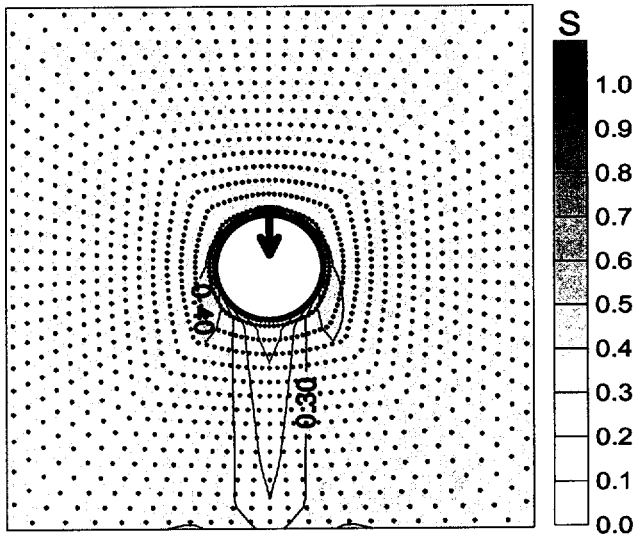

Figure 5. Saturation contours and location of first drip with the refined unstructured grid u2

α = 1.0E-5 Pa^{-1}, results from the numerical simulations over-predict dripping threshold and this error increases with α. Percent error compared to the analytical solution for rectangular and unstructured grids is shown in Figure 7. Error resulting from the unstructured grids approaches zero as α becomes small. The unstructured grid is also apparently sensitive to grid refinement. Error increases markedly with α for grid u0. Refinement with two additional rings of nodes in the region adjacent to the drift wall boundary (grid u2) resulted in an error of 49% for α = 3.3E-3 Pa^{-1}. Error with the rectangular grids also increases with α but less than the unstructured grid u0. For the rectangular grids, error also becomes negative at small α.

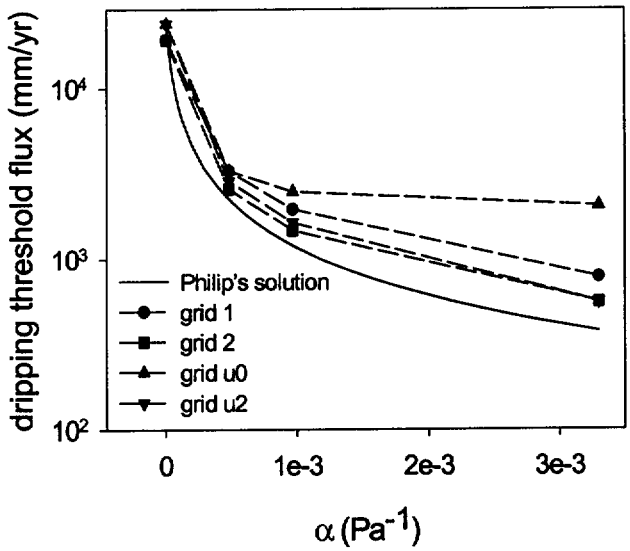

Figure 6. Dripping threshold as a function α obtained from numerical simulations compared to the analytical solution of Philip et al. (1989).

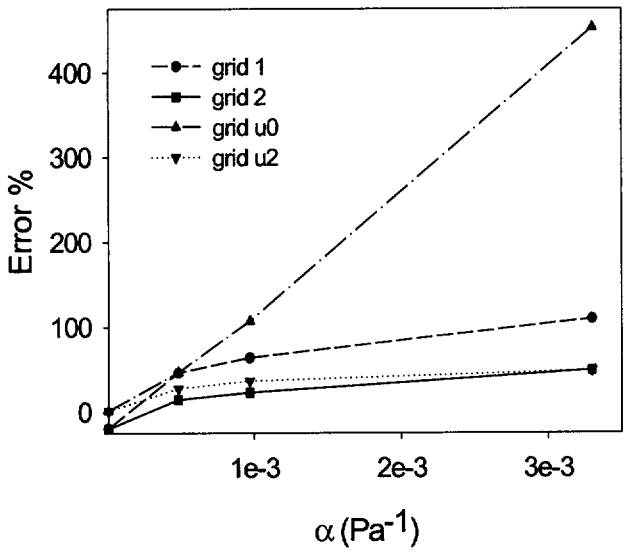

Figure 7. Percent error resulting from numerical simulations as compared to the analytical solution.

DISCUSSION

The presence of an underground opening creates a boundary layer at the drift wall with sharp gradients in pressure and saturation, as shown in Figures 1, 2, and 5. The thickness of this boundary layer is proportional to α^{-1} and is on the order of 3 cm for α = 3.3E-3 Pa^{-1}. It follows that to obtain an accurate numerical solution, node spacings in this region must be smaller than the boundary layer thickness in order to resolve the sharp gradients. The effect of grid refinement is clearly shown by the dramatic reduction in error obtained from grid u2 as compared with grid u0. Attempts at further grid refinements within the boundary layer formed by α =3.3E-3 Pa^{-1}, however, resulted in increased error apparently caused by truncation to fixed decimal formats in the meshing and input formatting codes.

Rather surprisingly, the ad hoc arrangement of nodal connections in the rectangular elements defining the drift wall boundary, as detailed in Figure 3 and Table 1, results in comparatively reasonable error over the range of α values considered here. The first drips form and leakage into the drift subsequently develops at nodal connections away from the crown of the drift. The theoretical analysis by Philip et al. (1989) shows that, for a horizontal cylindrical opening, the first drips form when a saturation of 1 is attained at the top center crown of the drift. In this respect, the unstructured grids with the drift wall defined by a circular boundary are consistent with theory. In the rectangular element grids 1 and 2, the elements above the drift crown remain unsaturated while leakage into the drift occurs from elements away from the drift crown. This suggests the possibility that additional nodal connection adjustments could further reduce the error and result in a better match to theory both in location and threshold for dripping. Grids with rectangular elements have the advantage of simplicity in assigning property values from random field generation for heterogeneous models. Future work with the unstructured grids will involve defining the drift by a change in material properties to estimate not just dripping threshold but also flow rate into the drift after the threshold has been exceeded. An unstructured grid will probably be necessary to accurately characterize the effects of irregularities in drift shape, perhaps due to partial drift collapse, on seepage into waste emplacement drifts.

REFERENCES

Birkholzer, J., G. Li, C.-F. Tsang and Y. Tsang, 1999. Modeling studies and analysis of seepage into drifts at Yucca Mountain, *J. Cont. Hydr. 38(1-3)*, p349-384.

U.S. Department of Energy, 1998. Viability Assessment of a Repository at Yucca Mountain. DOE/RW–0508. Washington, DC, U.S. Department of Energy

Gardner, W.R. 1958. Some steady state solutions of unsaturated moisture flow equations with application to evaporation from a water table. *Soil Science* 85: 228–232.

Haukwa, C., 1998, AMESH: A mesh creating program for the integral finite difference method, Earth Sciences Division Ernest Orlando Lawrence National Laboratory Berkeley, California, 55p.

Lichtner, P.C., and M.S. Seth. 1998. MULTIFLO User's Manual, MULTIFLO Version 1.2β: Two-phase nonisothermal coupled thermal-hydrologic-chemical flow simulator. San Antonio, TX: Center for Nuclear Waste Regulatory Analyses.

Philip, J.R., J.H. Knight, and R.T. Waechter 1989, Unsaturated seepage and subterranean holes, conspectus, and exclusion problem for circular cylindrical cavities. Water Resources Research 25(1), 16–28.

ACKNOWLEDGMENTS

This report was prepared to document work performed by the Center for Nuclear Waste Regulatory Analyses for the Nuclear Regulatory Commission under Contract No. NRC 02-97-009. The report is an independent product of the CNWRA and does not necessarily reflect the views or regulatory position of the NRC.